The EMBO Journal Vol. 22 No. 14 pp. 3591–3601, 2003

The mechanism of internalization of glycosylphosphatidylinositol-anchored prion protein

Claire Sunyach[1], Angela Jen, Juelin Deng, Kathleen T.Fitzgerald[2], Yveline Frobert[3], Jacques Grassi[3], Mary W.McCaffrey[2] and Roger Morris[4]

Molecular Neurobiology Group, MRC Centre for Developmental Neurobiology, King's College London Guy's Campus, London SEI 1UL, UK, [2]Cell and Molecular Biology Laboratory, Biochemistry Dept, UCC Cork, Ireland and [3]Service de Pharmacologie et d'Immunologie, CEA/Saclay, 91191 Gif sur Yvette, France

[1]Present address: IPMC du CNRS, UPR411, 660 Route des Lucioles, 06560 Valbonne, France

[4]Corresponding author
e-mail: roger.morris@kcl.ac.uk

The mode of internalization of glycosylphosphatidylinositol-anchored proteins, lacking any cytoplasmic domain by which to engage adaptors to recruit them into coated pits, is problematical; that of prion protein in particular is of interest since its cellular trafficking appears to play an essential role in its pathogenic conversion. Here we demonstrate, in primary cultured neurons and the N2a neural cell line, that prion protein is rapidly and constitutively endocytosed. While still on the cell surface, prion protein leaves lipid 'raft' domains to enter non-raft membrane, from which it enters coated pits. The N-terminal domain (residues 23–107) of prion protein is sufficient to direct internalization, an activity dependent upon its initial basic residues (NH_2-KKRPKP). The effect of this changing membrane environment upon the susceptibility of prion protein to pathogenic conversion is discussed.

Keywords: coated pits/endocytosis/GPI/lipid rafts/sphingolipids

Introduction

Prion protein is a glycosylphosphatidylinositol (GPI)-anchored glycoprotein (Stahl *et al*., 1987) abundantly expressed on neurons, neuroendocrine cells and stromal cells of the lymphoreticular system (Ford *et al*., 2002a,b). The conformational conversion of normal cellular prion protein (PrP^C) into a protease-resistant, amyloidogenic conformation (PrP^{res}) is the defining step in prion infection (Prusiner, 1998) for which expression of PrP^C is both required and rate limiting (Büeler *et al*., 1993; Weissmann *et al*., 2001).

Efficient transfer of infection requires direct contact between infected and target cells (Kanu *et al*., 2002), although the conversion of PrP^C to pathogenic PrP^{res} may occur in a post-plasma membrane compartment (Caughey and Raymond, 1991; Caughey *et al*., 1991; Borchelt *et al*., 1992). PrP^C cycles between the cell surface and endosomal compartments, a process thought to be critical to both its normal and pathogenic function (Harris, 1999). The GPI anchor of PrP^C determines its route of internalization and is necessary for the propagation of infection (Taraboulos *et al*., 1995; Kaneko *et al*., 1997).

Although PrP^C can be converted in cell-free systems into a protease-resistant form (Caughey *et al*., 2001), no one has yet produced infectious PrP^{res} by this means (Chesebro, 1998; Hill *et al*., 1999). It appears that some cellular mechanism is necessary to chaperone the formation of infectious PrP^{res}, where the interaction of the PrP^C/PrP^{res} complex with the hydrophobic environment of the membrane, or the pH drop accompanying endocytosis, are favoured candidates since both affect the conformation of recombinant PrP (Morillas *et al*., 1999; Alonso *et al*., 2001; Sanghera and Pinherio, 2002).

On the cell surface, PrP^C is found within 'rafts' (Kaneko *et al*., 1997; Naslavsky *et al*., 1999; Baron *et al*., 2002), microdomains formed in the membrane by the condensation of saturated sphingolipids with cholesterol to produce an ordered lipid environment that corrals GPI-anchored, but excludes most transmembrane, proteins (Simons and Ikonen, 1997). This ordered lipid environment is insoluble in non-ionic detergents, providing a simple indicator of whether a particular protein is within raft or non-raft membrane (Brown and Rose, 1992).

The rafts enclosing PrP^C on neurons are distinctive, being more soluble than and enclosing a different set of proteins from those that surround Thy-1, the major neuronal GPI-anchored protein (Madore *et al*., 1999). Moreover a significant proportion of PrP^C (but not Thy-1) is fully soluble in non-ionic detergents (Madore *et al*., 1999) and cannot be within a raft as classically defined (Simons and Ikonen, 1997).

The pH encountered by a protein depends on its route of intracellular trafficking: recycled proteins such as the transferrin receptor (TfR) rapidly exit early endosomes (pH 5.8 ± 0.2) to enter less acidic (pH 6.2) tubulovesicular recycling endosomes, whereas proteins destined for degradation pass into more acidic (pH ~5) late endosomes and lysosomes (Gagescu *et al*., 2000). Internalized GPI-anchored proteins can be routed along either of these paths depending upon the cell type in which they are expressed (Fivaz *et al*., 2002).

The route and mechanism of internalization of PrP^C are controversial. Seminal studies by Harris and colleagues showed that chicken PrP^C transfected into mouse N2a neuroblastoma cells was internalized via coated pits (Shyng *et al*., 1994) in a process dependent upon its N-terminal domain (Shyng *et al*., 1995a; Nunziante *et al*., 2003). Subsequent studies (Kaneko *et al*., 1997; Marella *et al*., 2002), also using N2a cells, have argued that mammalian PrP^C is internalized by one of the non-coated pit mechanisms characterized for raft-associated proteins

(Lamaze *et al*., 2001; Puri *et al*., 2001; Sabharanjak *et al*., 2002). Relatively high levels (≥100 μM) of Cu^{2+}, binding to histidine residues in the octapeptide repeat region of the N-terminal domain of PrP^C (Perera and Hooper, 2001), have been found to stimulate (in N2a cells; Pauly and Harris, 1998) or be required for (in SH-SY5Y cells; Perera and Hooper, 2001) endocytosis of transfected PrP^C. However, Nunziante *et al*. (2003) have shown that mouse PrP^C in which the N-terminal domain has been substituted by the non-Cu^{2+}-binding *Xenopus* homologue is endocytosed on N2a cells.

We have investigated the endocytosis of endogenously expressed mouse PrP^C on primary cultured adult mouse sensory neurons, and on N2a cells. Thy-1, the major GPI-anchored protein of adult neurons (Morris, 1992), has been used as a control GPI-anchored protein. TfR, the prototypical transmembrane protein endocytosed by coated pits (e.g. Gagescu *et al*., 2000) and excluded from lipid rafts (e.g. Shogomori and Futerman, 2001), has been used as a positive control, supplemented in fluorescence by the low-density lipoprotein receptor (LDL-R) which is similarly well established as a non-raft protein that is endocytosed via coated pits (Matter *et al*., 1994; Czekay *et al*., 2001).

Results

PrP^C but not Thy-1 is rapidly endocytosed by sensory neurons

Immunofluorescent labelling of cultured neurons, distinguishing surface (green) from internal (red) antigen (Figure 1A and B) demonstrated a marked difference in cellular distribution between the two GPI proteins: virtually all Thy-1 was located on the cell surface, whereas the majority of PrP^C was located intracellularly.

To investigate the contribution of endocytic trafficking to the intracellular pool of PrP^C, monovalent antibody reagents (see Supplementary data available at *The EMBO Journal* Online) were used to label endogenous PrP^C and Thy-1 for fluorescence and electron microscopy. To optimize image capture to enable detection of the low

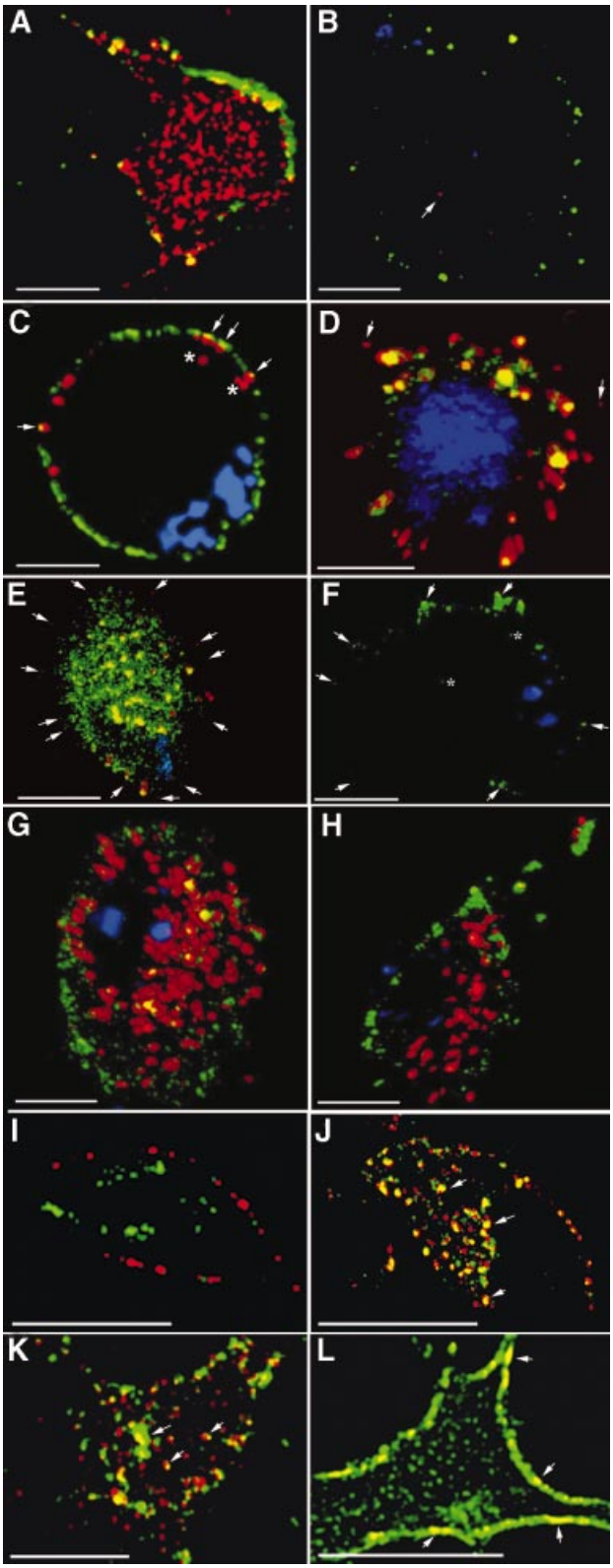

Fig. 1. Kinetics and mechanism of endocytosis of PrP^C. (A and B) PrP^C (**A**) but not Thy-1 (**B**) is mostly intracellular. Sensory neurons, labelled at 10°C with Alexa 488 (green)-coupled Fab, were fixed, permeabilized and re-labelled with Alexa 594 (red) Fab to differentiate between external and internal protein. Sections in (A) are several μm below the nucleus, near the adherent surface, and show internal PrP^C in tubular structures. Thy-1 sections in (B) are just below the nucleus; the arrow points to internal Thy-1. (**C**–**E**) Co-labelling of neurons for PrP^C (Alexa 488–Fab) and TfR (Texas red–Tf) at 10°C, followed by incubation at 37°C for 0 (C) or 2 (D and E) min. Arrows in (C) point to TfR underlying PrP^C at or near the surface. The asterisks indicate TfR that is clearly internal. Cells with low (D) and high (E) levels of PrP^C have internalized 95.9 and 91.4%, respectively, of their surface label; arrows point to weak label remaining at the cell surface. (**F**) Labelling for Thy-1 (green) after 6 min at 37°C; arrows show surface label, asterisks show internalized label (4.8% of the total). TfR is not shown as it overlies and hides internalized Thy-1. (**G** and **H**) PrP^C trafficking, pulsed on the surface with Alexa 488 (green) Fab, chased at 37°C with Alexa 594 (red) Fab for 10 min (G; 28.2% green Fab on surface) or 15 min (H; 83.7% on surface). (I–L) Dual labelling of N2a cells after 15 min internalization at 37°C of directly coupled Fab labelling endogenous PrP^C (green), and either Thy-1 (red) in its native (**I**) and fusion PrP^{107}–Thy-1 (**J**) forms, or the 3F4 epitope on cells expressing 3F4-tagged PrP (**K**) or N-terminally mutated 3F4-tagged PrP (**L**). Arrows in (J) and (K) point to examples of co-labelling of internal tubulovesicular structures, in (L) to dual label for PrP^C and N-terminally mutated PrP at the cell surface, whereas only label for PrP^C has been internalized. Throughout, a 200 nm *z*-axis series of images has been collected and volume deconvolved, and 10 (neurons) or four (N2a cells) sections reassembled and fluorescence in different compartments measured using Volocity (Improvision) software. Scale bars are 10 μm.

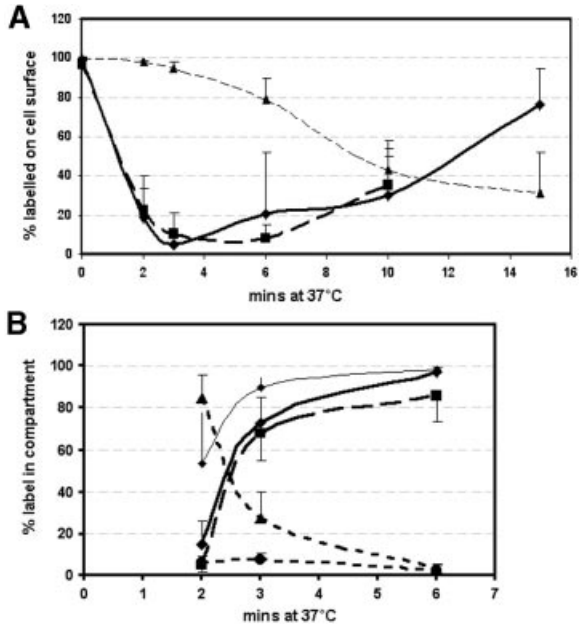

Fig. 2. Kinetics of internalization of PrP^C, Thy-1 and TfR by sensory neurons. (**A**) Percentage surface label for: PrP^C, diamonds (solid line); Thy-1, triangles; TfR, squares. (**B**) Percentage of internalized label in different compartments, showing: PrP^C within tubules, diamonds (bold line); PrP^C co-localized with TfR within tubules, squares (bold dashed line); TfR within tubules, diamonds (thin line); PrP^C in endocytic vesicles, triangles (dashed line); PrP^C co-localized with TfR in endocytic vesicles, circles (dashed line). Mean ± SD, 6–16 cells analysed at each point. Labelled structures >5 voxels (0.01 μm^3) have been taken as tubular; and smaller structures (mostly 1 voxel) as endocytic vesicles. The tubules visible in Figure 1 are 0.1–1.2 μm^3 in the 2 μm slice sampled.

intensity of label for endogenous PrP^C (<10% that of TfR, itself expressed at low levels on post-mitotic neurons compared with cell lines), following incubation at 37°C for different time points, cells have been fixed and coverslipped.

TfR was, as expected, rapidly endocytosed and transported to large tubulovesicular recycling endosomes (Figures 1D and E, and 2). PrP^C was internalized almost as quickly, with proportions similar to TfR internalized after 2 and 3 min (Figure 2A). Two observations suggested that endocytosis of TfR was slightly faster: at 0 min (after 10 min pre-inubation at 10°C), label for TfR underlay PrP^C at the cell surface, and occasionally some labelled TfR but not PrP^C was clearly within the cell (Figure 1C); and more internalized TfR was in tubular structures at 2 min (Figure 2B; $P = 0.01$). Within tubules, almost all PrP^C co-localized with TfR (Figure 2B); the small amount that did not was at outer layers of tubules whose core was intensely labelled for both (e.g. Figure 1E).

Co-localization of PrP^C and TfR in early endosomes, prior to their arrival in recycling tubules, would be stronger evidence that the two proteins are endocytosed together. Although early endocytic vesicles are too small to be resolved in the light microscope, at 2 min internalized fluorescence was dominated by very small objects (>95% were 1 voxel, 0.002 μm^3) that rapidly formed tubules (Figure 2B). We assume these to be early endocytic vesicles. The majority were labelled either for PrP^C or TfR; only 6% of PrP^C vesicles co-labelled for TfR

Table I. Extent of co-localization of proteins in vesicles ⩽ 0.01 μm^3 (5 voxels) after 2 min endocytosis

	PrP with TfR	LDL-R with TfR	PrP with LDL-R
% endocytosis	92.4 ± 6.4 and 83.5 ± 10	90.6 ± 5.7 and 86.3 ± 3.2	93.1 ± 4.1 and 91.9 ± 1.5
% co-localized	6.1 ± 3.4	5.9 ± 2.2	0.7 ± 3.4

(Figure 2B). To determine the degree of co-localization expected for receptors internalized by the same mechanism (coated pits), internalization of the LDL-R was compared with that of TfR and PrP^C. The intensity of label for LDL-R ($1–5 \times 10^5$ fluorescent units per 0.2 μm optical section) was similar to PrP^C, 10% that of TfR. LDL-R was endocytosed as fast as TfR and PrP^C, and showed an identical level of co-localization with TfR in early endosomes (Table I). The 6% co-localization of PrP^C with TfR was therefore in the range expected for proteins expressed at this level and internalized via coated pits. Co-localization of PrP^C with LDL-R was 10 times lower, in keeping with the lower level of LDL-R labelling.

The rate of recycling of PrP^C to the cell surface also mirrored that of TfR. For PrP^C, recycling was assessed by pulse–chase labelling (green Fab anti-PrP bound at 10°C chased with red Fab at 37°C). Recycling of green Fab to the cell surface, first detected in a few cells after 6 min (Figure 2A), reached substantial levels in all by 10 min (Figures 1G and 2A); by 15 min, the green Fab was either predominantly on the cell surface (Figure 1H) or had already started to be re-internalized. Endocytosed Tf returned to the surface as apo-Tf is released, allowing its receptor to bind fresh Texas red–Tf; adding fresh Texas red–Tf to the medium at the beginning of the 37°C incubation labelled recycled TfR on the surface (Figure 2A). As with PrP^C, cells with recycled TfR were first seen after 6 min, with all cells showing clear surface label at 10 min.

In contrast to the rapid trafficking of PrP^C and TfR, Thy-1 was slower (Figure 2A). Internalized label was first detected within small vesicles and tubules (Figure 1F) that co-labelled with TfR. No internalized Thy-1 label was found in cortical tubulovesicular structures devoid of TfR label described for some GPI-anchored proteins (Sabharanjak *et al*., 2002).

The early stages of endocytosis of PrP^C, labelled with Fab–5 nm gold, were examined in the electron microscope. After 2 min incubation at 37°C, PrP^C label was found in ~5%, and TfR in <1%, of coated pits and coated vesicles (Figure 3A–E), proportions that decreased ~10-fold thereafter. Occasional co-labelling of PrP^C and TfR within or adjacent to a coated pit or vesicle was found (Figure 3A and E). In contrast, Thy-1 label was not found within coated vesicles; it was occasionally seen at the lip of a coated pit, but not within its concavity, in agreement with previous studies (Lemansky *et al*., 1990; Bamezai *et al*., 1992; Tiveron *et al*., 1994; Madore *et al*., 1999).

Even in mitotic cells expressing high levels of TfR, only a few percent are within coated pits, most being clustered in regions above clathrin lattices (Lamaze *et al*., 2001). On sensory neurons, although >95% of PrP^C was not

associated with TfR, the converse was not true: TfR was readily found within or beside clusters of PrP^C, whether in 80–100 nm thick cross-section (Figure 3F–H) or in oblique sections providing an *en face* view of the surface (Figure 3I–K). TfR was significantly associated with PrP^C but not Thy-1 (Figure 4A).

Larger sectors of the membrane, immunolabelled on both sides, were examined using the 'tear-off' technique (Sanan and Anderson, 1991). When applied to neurons labelled externally for PrP^C and internally for the clathrin adaptor AP2 (10 nm gold; Figure 3L–P), virtually all AP2 was associated with structures that appeared (from the perspective of looking down on the cytoplasmic surface) to be 'raised'. Although isolated 'hillocks' of these structures occurred, they more usually formed networks of tubular structures. At 0 min, 90.3 ± 8.7% of AP2 was on a raised structure, as was 50.1 ± 25.6% of PrP^C and 2.2 ± 5.8% of Thy-1 (all three values differ, $P \leqslant 0.0001$; 30 fields counted). In some preparations, the electron density of the membrane surface obscured the raised structures, but co-localization of AP2 over clusters of PrP^C was readily found (Figure 3Q). Some PrP^C label on flat areas was sufficiently distant from AP2 to suggest it was

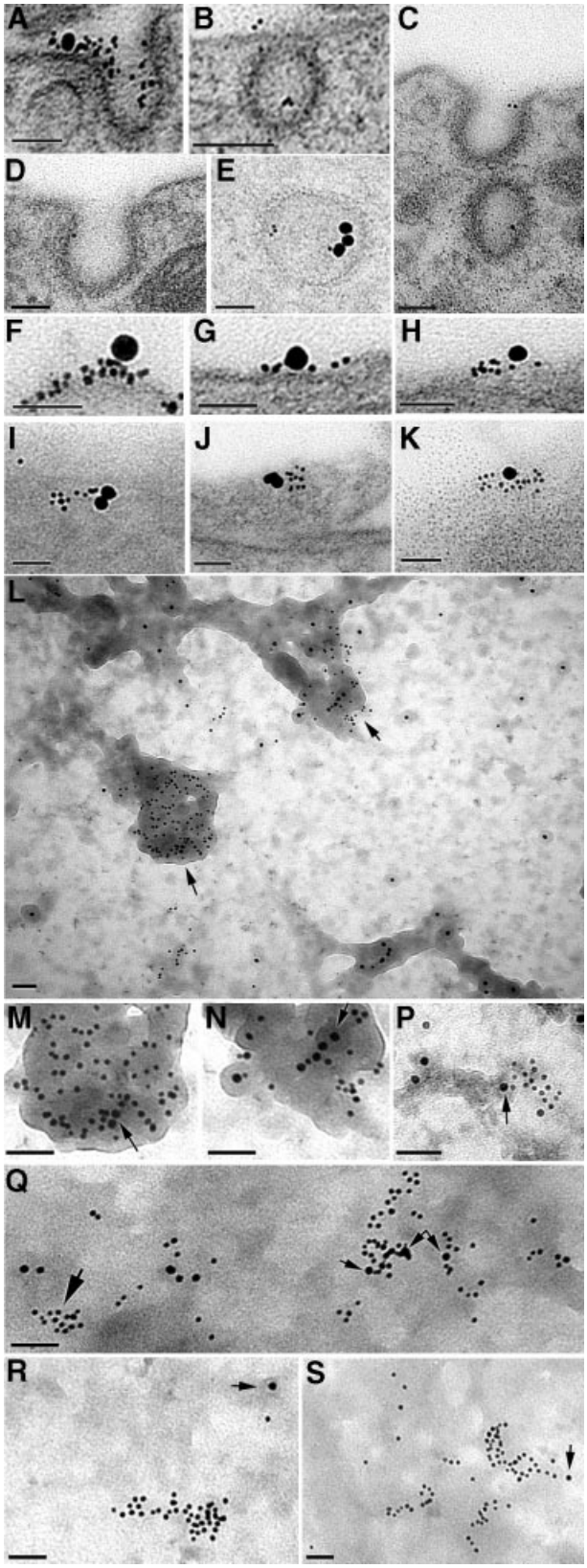

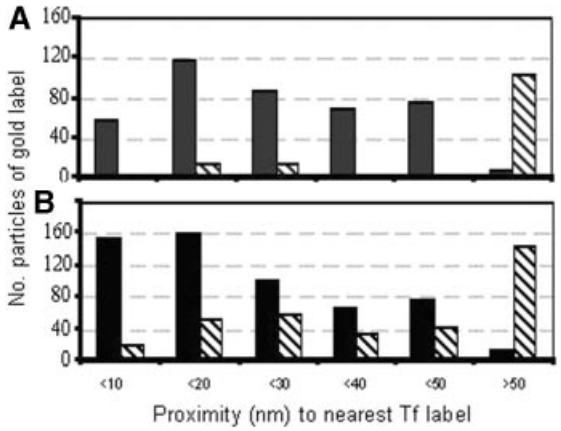

Fig. 4. Proximity of label for PrP^C (black) and Thy-1 (stripes) to labelled TfR on the surface of neurons (**A**) or N2a cells (**B**). Cells were double labelled at 10°C for TfR (20 nm gold) and either PrP^C or Thy-1 (5 nm gold). The numbers of 5 nm gold particles falling within a ring of the stated radius from the edge of the nearest TfR label were counted (at 100 000× magnification); where no PrP^C or Thy-1 occurred within 50 nm of a TfR cluster, a single count was recorded (>50 nm). The distribution of label within 50 nm of TfR differed significantly between PrP and Thy-1 for neurons ($P < 0.001$; $n = 110$) and N2a cells ($P < 0.05$, $n = 150$).

Fig. 3. PrP^C immunolabelling of sensory neurons, seen by transmission electron microscopy of sectioned material (A–K) or of tear-off samples of the cell surface (L–S), using anti-PrP Fab directly coupled to 5 nm gold with biotinylated Tf coupled to 20 nm avidin–gold (A–K) or AP2 labelled with 10 nm gold (L–S). (**A–E**) Examples of PrP^C entering coated pits or vesicles after 2 min at 37°C, with occasional co-localization with TfR (A and E). (**F–K**) Co-localized TfR and PrP on the cell surface. (**L**) Overlapping PrP and AP2 at electron-dense cytoplasmic tubular structures (**M** and **N**) Regions arrowed in (L) at higher power; arrows in (M) and (N) point to 10 nm AP2 label. (**P**) A cluster of PrP^C partially overlapping an AP2-labelled electron-dense region (arrowed). (**Q**) Clusters of PrP^C overlying AP2 (small arrows), with another PrP^C cluster (large arrow) not associated with AP2. In this sample, the cytoplasmic surface is less distinct (presumably masked by cytoplasmic protein), somewhat obscuring the AP2-positive electron-dense structures. (**R** and **S**) Examples of clusters of PrP not associated with AP2 label (the nearest AP2 label is arrowed). Scale bars are 50 nm.

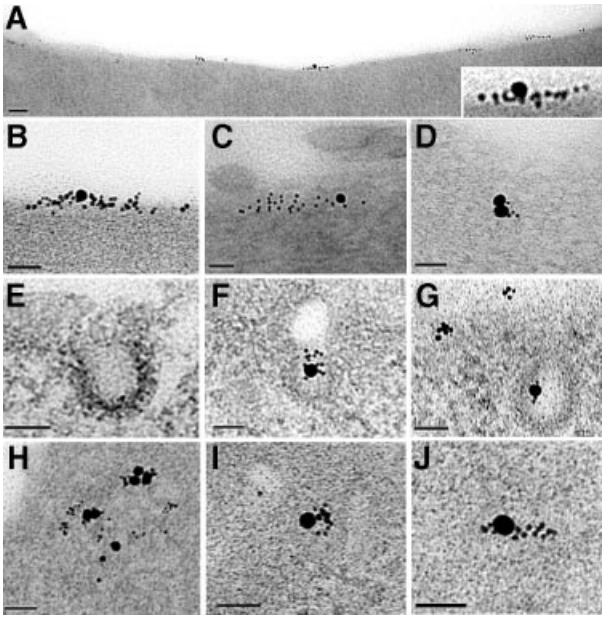

Fig. 5. Endocytosis by N2a cells of PrP^C (5 nm gold) and TfR (20 nm gold). (**A–D**) Co-labelling of clusters of PrP^C and TfR on the cell surface in transverse (A, higher power view of co-labelled cluster in inset) and oblique (C and D) sections. (**E–G**) PrP^C in coated pits (in these cells coated pits often came off trabeculae as in F) or coated vesicle [G; clusters of PrP^C (upper left) are on the cell surface]. (**H–J**) PrP^C co-localized with TfR in intracellular vesicles after 2 min incubation. The electron-dense cytoplasm of these cells obscured the vesicular membrane. Scale bars are 50 nm.

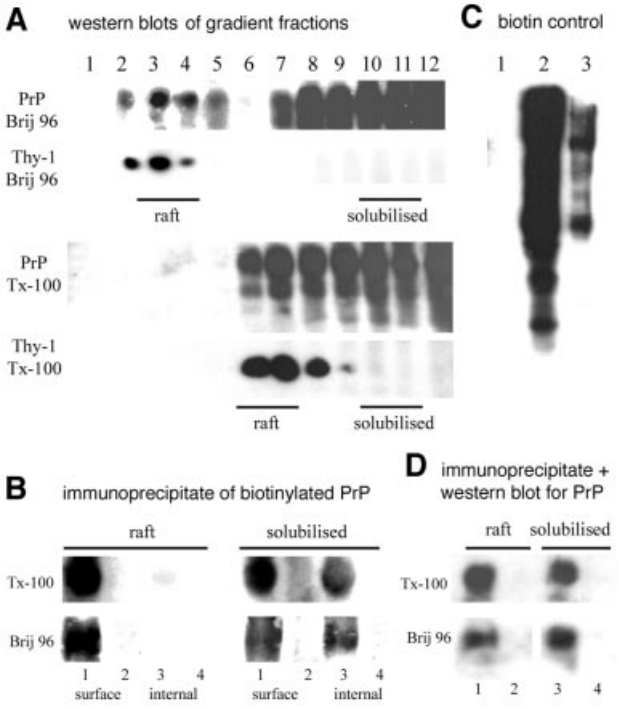

Fig. 6. Much cell surface, and all endocytosed, PrP^C on N2a cells is in membrane that is fully solubilized in Brij 96 and Triton X-100. (**A**) Western blot of PrP^C and Thy-1 in density gradient fractions after solubilization in 0.5% Brij 96 or Triton X-100. Fractions pooled for the raft and fully solubilized fractions are indicated. (Rafts float at lower density in Brij 96 than Triton X-100; Madore *et al*., 1999.) (**B**) Cells reacted with disulfide-linked biotin were either solubilized immediately ('surface') in Brij 96 or Triton X-100, or first incubated for 15 min at 37°C before surface biotin was stripped by reductive cleavage ('internal') and then solubilized. PrP^C in pooled raft/solubilized fractions was immunoprecipitated and visualized by streptavidin–horseradish peroxidase (HRP). Lanes 1 and 3, immunoprecipate; lanes 2 and 4, post-precipitate supernatant. (**C**) Controls for reductive cleavage. Electrophoresed samples probed with streptavidin–HRP were: 1, biotinylated cells cleaved with glutathione; 2, cells biotinylated only; and 3, cells biotinylated, incubated for 15 min at 37°C then cleaved with glutathione. (**D**) Confirmation by western blot that immunoprecipitation of PrP^C in (B) was quantitative: lanes 1 and 3, immunoprecipitate; lanes 2 and 4, post-precipitate supernatant.

raft, rather than clathrin, associated (Figure 3R and S). PrP^C clusters partially overlapping AP2 hillocks and flat, AP2-negative areas possibly indicated the transition from raft to non-raft area (Figure 3P). Such movement of PrP^C but not Thy-1 was apparent quantitatively: from 0 to 2 min incubation, the proportion of PrP^C >250 nm distant from AP2 decreased from 71.5 ± 6.5 to 28.5 ± 7.7% ($P \leqslant 0.0001$), whereas that of Thy-1 remained stable (44.7 ± 9.5 and 45.9 ± 9.7%, $P = 0.68$).

In these studies (and those described below for N2a cells), no Cu^{2+} was added to the medium, which was the same as that used with transfected cells in which 100 μM Cu^{2+} was required for endocytosis of PrP^C (Perera and Hooper, 2001). Addition of the copper chelator bathocuproine disulfonic acid at high concentrations (⩾200 μM) inhibited PrP^C internalization in some cells, but equally inhibited TfR uptake by the same cells, whose shrunken appearance suggested that the inhibition was pathological rather than physiological. Lower concentrations (2 and 20 μM) of chelator did not affect internalization of PrP^C or TfR (data not shown), suggesting that the rapid and complete endocytosis of neuronal PrP^C was not dependent upon trace levels of Cu^{2+} inadvertently present in our preparation.

PrP^C is also endocytosed via coated pits on N2a cells

Primary cultures, in which a few hundred adult sensory neurons grow axons over a substrate of Schwann cells and fibroblasts, are not suitable for biochemical analysis. We therefore assessed whether N2a cells, which have been widely used to study the trafficking of transfected PrP^C, reproduced the neuronal difference in surface localization and trafficking of Thy-1 and PrP^C. Thy-1 is not expressed endogenously by N2a cells; we therefore expressed it by transfection and selected by flow cytometry a polyclonal population that expressed surface levels of Thy-1 comparable with their level of endogenous PrP^C. As with brain membranes (Madore *et al*., 1999), endogenous mouse PrP^C on the N2a cells was more soluble than Thy-1 (Figure 6A); and PrP^C but not Thy-1 was endocytosed by these cells (Figures 1I and 8). They therefore seemed an acceptable model for the membrane organization and trafficking of both GPI-anchored proteins.

Endogenously expressed PrP^C was endocytosed on N2a cells more slowly than on sensory neurons, with ~25% internalized within 10 min (Figures 5, 7C and 8; cf. Shyng *et al*., 1993). TfR on the cell surface was again significantly associated with PrP^C but not Thy-1 (Figures 4B and 5A–D). TfR and PrP^C occurred frequently within coated pits and vesicles (Figure 5E–G). Double labelling for PrP^C and TfR was readily found at all stages

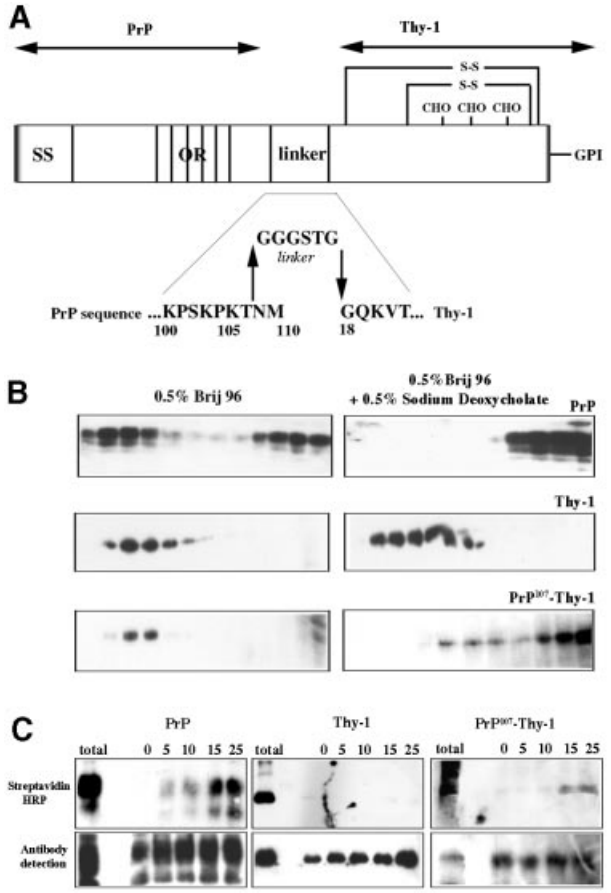

Fig. 7. The N-terminal domain of PrP^C is sufficient to specify the solubility and endocytosis of a GPI-anchored protein. (**A**) Scheme showing the fusion protein PrP^{107}–Thy-1, in which the N-terminal domain of PrP^C is joined via a flexible linker to full-length Thy-1. SS, signal sequence of PrP; OR, octapeptide repeats; CHO, the N-linked carbohydrate chains of Thy-1; S-S, disulfide bonds of Thy-1. Amino acids are abbreviated in single letter code. (**B**) Western blots of density gradient fractions after solubilization of N2a cells in Brij 96 with (right) or without (left) 0.5% sodium deoxycholate, probed for PrP^C, Thy-1 or fusion PrP^{107}–Thy-1. (**C**) Endocytosis measured by protection of biotinylated protein from extracellular reductive cleavage. N2a cells were surface biotinylated, and either solubilized immediately (total) or incubated at 37°C for the number of minutes indicated before external biotin was removed by glutathione cleavage; endogenous PrP^C (left) and Thy-1 (middle) or fusion PrP^{107}–Thy-1 (right) were immunoprecipitated and detected using streptavidin–HRP (upper panel) or western blotting (lower panel).

of intracellular trafficking, from coated pits and vesicles, through small vesicles to tubulovesicular structures (Figure 5). The route of endocytosis of PrP^C on N2a cells appeared, therefore, to reproduce that followed on neurons, although with slower kinetics. Endocytosis of Thy-1 was too slow to be detected over 15–25 min.

Is a fraction of surface PrP^C outside lipid rafts?

Since the TfR is used as the prototypical non-raft protein, could a proportion of PrP^C be outside rafts? We have used insolubility in Brij 96 as a criterion of raft association, since it has particular advantages for isolating neuronal rafts (Madore *et al*., 1999); however, insolubility of protein in Triton X-100 has long been accepted as

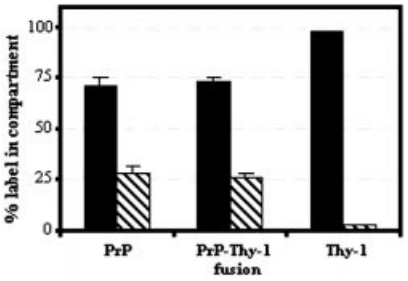

Fig. 8. Distribution of 5 nm gold–Fab detecting PrP, PrP^{107}–Thy-1 (Fusion) and Thy-1 on the cell surface (black) and within intracellular vesicles (stripes) on N2a cells after 10 min incubation at 37°C. The percentages of labelled PrP^C and fusion protein on the cell surface and within intracellular vesicles were similar ($P = 0.57$ and 0.64, respectively) and differed from Thy-1 ($P < 0.0001$).

indicative of raft association (Brown and Rose, 1992; Simons and Ikonen, 1997).

A substantial proportion of brain PrP^C, but not Thy-1, is fully solubilized in both Brij 96 and Triton X-100 (Madore *et al*., 1999; and Supplementary data). For N2a cells also, ~50% of PrP^C was found in the fully solubilized fraction after extraction with either Brij 96 or Triton X-100, in contrast to Thy-1, >99% of which floated in the raft fraction (Figure 6A). The soluble (non-'raft') PrP^C undoubtedly includes some newly synthesized protein in the endoplasmic reticulum (ER), which does not become incorporated into detergent-resistant domains until a late Golgi compartment (Brown and Rose, 1992). To identify specifically surface PrP^C, N2a cells were biotinylated with membrane-impermeant reagent at 4°C, solubilized in Brij 96 or Triton X-100, floated on a sucrose density gradient, and the raft and fully solubilized membrane fractions immunoprecipitated to identify biotinylated PrP^C present in each fraction. Both detergents fully solubilized ~30–50% of surface PrP^C, with the remainder in the raft fraction (Figure 6B).

To evaluate the solubility of endocytosed PrP^C, after biotinylation at 4°C, cells were held at 37°C for 15 min, then residual surface biotin removed by reductive cleavage at 4°C prior to solubilization and gradient centrifugation. Immunoprecipitation revealed that >95% of biotinylated PrP^C, protected from reductive cleavage by being internalized (Figure 6C), was recovered in the fully solubilized fraction (Figure 6B).

A significant proportion of surface PrP^C, and virtually all internalized PrP^C, is therefore within a membrane environment that is fully solubilized by both Triton X-100 and Brij 96.

The N-terminus of PrP^C is sufficient to change the lipid environment, and drive endocytosis, of GPI-anchored Thy-1

During each cycle of its normal endosomal trafficking, a small fraction of PrP^C is cleaved around residue 110, leaving its residual C-terminal domain in the membrane; the truncated GPI-anchored protein devoid of its N-terminal domain is not endocytosed (Shyng *et al*., 1993). We find that this truncated C-terminal domain is less soluble than full-length PrP^C, having instead the insolubility characteristic of Thy-1 (see Supplementary data).

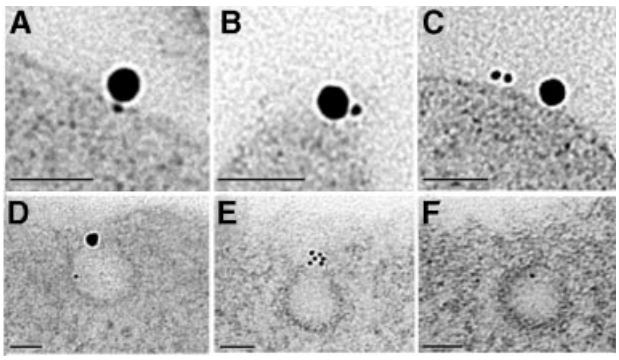

Fig. 9. Endocytosis of fusion PrP^{107}–Thy-1 by N2a cells after 2 min at 37°C. (**A–C**) Co-localized TfR and fusion protein on the cell surface. (**D–F**) Fusion protein in coated pits (D also contains a TfR label). Scale bars are 50 nm.

The N-terminal domain is therefore necessary for both the endocytosis of PrP^C and the degree of order of the lipids surrounding it. Is it sufficient? To examine this question, we substituted the C-terminal domain of PrP by linking its N-terminal 107 residues via a flexible six amino acid linker to full-length Thy-1 (PrP^{107}–Thy-1; Figure 7A), a protein with different trafficking properties but similar to the C-terminal domain of PrP^C in size (121 amino acids, compared with 111 of Thy-1), *N*-glycosylation and mode of membrane anchorage (Morris, 1992).

PrP^{107}–Thy-1 was expressed on the surface of stably transfected N2a cells; cells expressing ~25% the level of endogenous PrP^C were selected by flow cytometry to ensure that the fusion protein was present at trace levels and did not 'swamp' the lipid environment or protein interactions of endogenous PrP^C. The fusion protein was found in membrane domains that largely resisted solubilization in Brij 96 but were almost entirely solubilized in Brij 96/sodium deoxycholate (Figure 7B), characteristics of PrP^C rather than Thy-1 (Figure 7B). Unlike Thy-1 itself (Figures 1I and 7C), the fusion protein associated on the cell surface with TfR (Figure 9A–C) and was internalized via coated pits and coated vesicles (Figure 9D–F) to an extent similar to endogenous PrP^C on the same cells (Figure 8).

The N-terminal domain of prion protein is therefore sufficient to change both the membrane environment and trafficking properties of a foreign GPI-anchored protein to those more typical of full-length PrP^C.

A basic amino acid motif in the N-terminal domain of PrP^C is required for endocytosis

The N-terminal cluster of basic residues (NH_2-KKRPKP) is a candidate binding site for negatively charged proteoglycans that are known to stimulate endocytosis of PrP^C (Shyng *et al*., 1995b). We therefore substituted three of these basic residues (Figure 10A), retaining their size and hydrophilicity along with the dibasic N-terminal ^{23}K to ensure cleavage of the signal sequence. These substitutions were made on full-length mouse PrP internally epitope tagged by substituting the hamster PrP sequence at residues 109–112 so that the protein could be distinguished from endogenous mouse PrP^C by 3F4 monoclonal antibody (Kascsak *et al*., 1987). The native 3F4-tagged

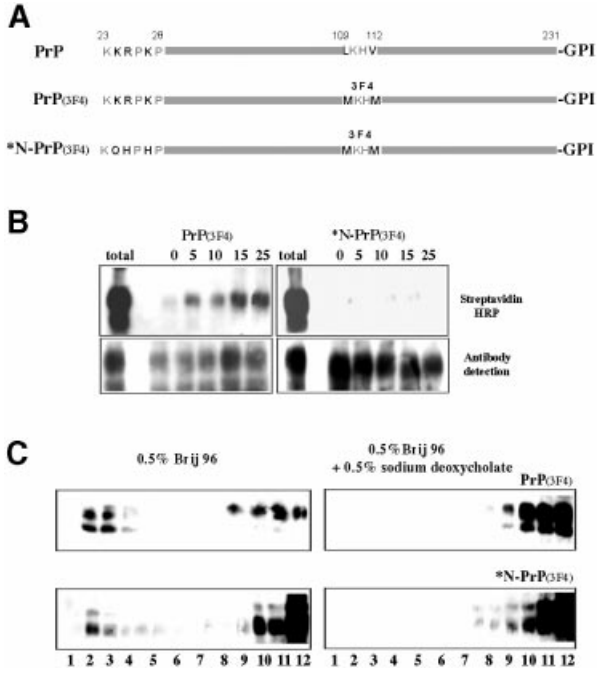

Fig. 10. Effect of diminishing the charge of the N-terminal cluster of basic amino acids on the internalization and solubility of 3F4-tagged PrP^C. (**A**) Scheme showing the mutations introduced to tag mouse PrP^C with the hamster 3F4 epitope, and then to mutate three N-terminal basic residues. (**B**) Endocytosis of 3F4-tagged PrP (left), and of N-terminally mutated *N-PrP (3F4 tagged) (right), measured by protection from reductive cleavage. (**C**) Western blots of native and N-terminally mutated PrP (3F4-tagged) after density gradient centrifugation, following solubilization in 0.5% Brij 96 with (left) or without (right) 0.5% sodium deoxycholate.

mouse PrP^C was indistinguishable from endogenous PrP^C in being endocytosed (Figure 10B), co-localizing with endogenous PrP^C (Figure 1K). However, the mutant protein was not endocytosed (Figure 10B) and by immunofluorescence remained almost entirely on the cell surface (Figure 1L), like Thy-1 rather than PrP^C (Figure 1I).

When the solubility of the mutant protein was analysed on sucrose gradients, it displayed the same characteristics as native epitope-tagged PrP^C (Figure 10C), suggesting that the signal within the N-terminal domain for endocytosis was separable from that directing the protein to a different lipid environment.

Discussion

PrP^C is generally thought of as a cell surface protein confined by its GPI anchor to sphingolipid rafts, from which it is endocytosed by a Cu^{2+}-activated mechanism, possibly to provide a Cu^{2+} uptake system (Harris, 1999; Brown, 2001). This study shows that endogenous neuronal PrP^C is endocytosed at a much faster rate than suggested by studies with transfected cell lines (Harris, 1999; Perera and Hooper, 2001; Magalhaes *et al*., 2002; Marella *et al*., 2002; Nunziante *et al*., 2003). It further demonstrates the following: (i) PrP^C leaves the detergent-insoluble 'raft' environment to cluster, along with the TfR, in non-raft membrane prior to endocytosis. PrP^C on the cell surface thus rapidly trafficks through two very different membrane

environments, possibly with very different consequences for its conformational stability. (ii) PrP^C is not endocytosed as a general function of its GPI anchor, but rather as a specific property of its N-terminal domain and in particular of its immediate N-terminal basic residues. (iii) Endocytosis of endogenous neuronal PrP^C does not require added Cu^{2+}; the physiological role of the trafficking of this protein may be wider than (or unrelated to) the uptake of this cation.

Route of endocytosis of PrP^C

Proof that a protein is internalized via a clathrin-independent mechanism can be relatively straightforward; if it is unaffected by the changes in cell metabolism induced by blocking clathrin-dependent internalization (changes resulting in cell death unless effective clathrin-independent mechanisms are rapidly activated; Damke *et al*., 1995; Sieczkarski and Whittaker, 2002; Wettey *et al*., 2002), then a coated pit-independent mechanism must be involved. The converse is not as easy to demonstrate. Failure to internalize a protein in a clathrin-blocked cell might be due to the cell's imminent demise; where induction of alternative mechanisms is sufficiently robust to spare the cell, there can be no guarantee that the pattern of internalization of the protein has not been altered.

Such considerations are particularly pertinent for PrP^C which, lacking a cytoplasmic domain that could bind directly to adaptor proteins, can only be internalized by binding to other endocytosed surface components such as lipid rafts or transmembrane proteins/proteoglycans. Such accessory components may not be present in amounts sufficient to drive the endocytosis of PrP^C overexpressed in a cell line, allowing alternative mechanisms (such as the Cu^{2+}-dependent mechanism; Perera and Hooper, 2001; Magalhaes *et al*., 2002) to come into play. We have therefore characterized the internalization of endogenously expressed PrP^C on neurons, the major cell type expressing this protein *in vivo* (Ford *et al*., 2002a,b).

On neurons, PrP^C is readily found within coated pits and coated vesicles, and associates with the TfR on the outer, and AP2 on the inner, surface of the membrane. PrP^C is transferred rapidly and directly to the recycling endosome and back to the cell surface with kinetics only marginally slower than those of the TfR, and distinctly faster than those of Thy-1. The trafficking of PrP^C thus clearly differs from the much slower, multistep clathrin-independent trafficking described for some other GPI-anchored proteins (Mayor *et al*., 1998; Chatterjee *et al*., 2001; Sabharanjak *et al*., 2002). Our results argue that PrP^C is internalized via coated pits into recycling endosomes from which it is rapidly retrieved to the cell surface. Green fluorescent protein (GFP)-tagged PrP^C (but not GPI–GFP) has been shown to be endocytosed via Rab5-containing early endosomes, implying a coated pit-mediated uptake of the hybrid protein (Magalhaes *et al*., 2002).

Our finding that endocytosed PrP^C is fully soluble in non-ionic detergents agrees with previous studies on the solubility of GPI-anchored proteins that are internalized via coated pits (Rijnboutt *et al*., 1996; Vilhardt *et al*., 1999) or are present in recycling endosomes (Fivaz *et al*., 2002); conversely, raft proteins that are internalized via clathrin-independent means remain in insoluble membrane in the process (Vilhardt *et al*., 1999; Lamaze *et al*., 2001). The egress of GPI-anchored proteins from rafts may be necessary in order to enter coated pits, since the structure of ordered lipid domains is unlikely to accommodate the tight curvature of coated pits/vesicles (Morris *et al*., 2003). What is remarkable about PrP^C is how rapidly it leaves its raft domains (or the raft domains break up around it) as its endocytic complex forms on the cell surface.

Trafficking role of the N-terminal domain of PrP^C

Shyng *et al*. (1995a) excised increasingly greater regions of the N-terminal domain (retaining ^{NH2}KK, with 3+ charges, throughout) and found a progressive reduction of up to 70% in PrP^C endocytosis. Nunziante *et al*. (2003) found that including all the basic motif in the deletion completely abrogated endocytosis. For both studies, it is unclear whether the excised region is inherently necessary for endocytosis, or acts in conjuction with the C-terminal domain. Our demonstration that PrP's N-terminal domain is sufficient to drive endocytosis, and determine the membrane microenvironment, of a foreign GPI-anchored protein (Thy-1) shows that both these properties are intrinsic to this domain.

Changing ^{NH2}KKRPKP to ^{NH2}KWHPHP, thereby lowering the charge of this motif from +5 to +2 on the cell surface (restored to +4 at pH 6 within endosomes), was a relatively subtle mutation that completely abrogated endocytosis. This motif forms part of a known binding site (Pan *et al*., 2002; Warner *et al*., 2002) for sulfated proteoglycans, major negatively charged groups on the cell surface that stimulate endocytosis of PrP^C (Shyng *et al*., 1995b), antagonize prion infection (Gilbert and Rudyk, 1999) and occur within prion plaques (McBride *et al*., 1998). We find (J.Deng, A.Jen and R.J.Morris, in preparation) that reduction of heparan sulfate on the surface of sensory neurons lowers the rate of endocytosis of PrP^C, suggesting that proteoglycans are part of the endocytic complex.

The rapid, constitutive and distinctive mode of internalization of PrP^C, dependent upon the phylogenetically conserved basic cluster of N-terminal residues (Simonic *et al*., 2000; Strumbo *et al*., 2001; Rivera-Milla *et al*., 2003), is presumably central to its normal function. This protein is notoriously 'sticky', binding to many proteins and surfaces, a property that may reflect a natural role as a component of a scavenger receptor complex, similar to that of another GPI-anchored protein, CD14 (Triantafilou and Triantafilou, 2002). Known scavenger receptors in the nervous system are expressed only on glia (Husemann *et al*., 2002); PrP^C may perform a scavaging function directly for neurons.

Pathogenic implications of PrP^C trafficking at the cell surface

Since the basic N-terminal motif we have identified as essential for the endocytosis of PrP^C is required for the pathogenic conversion of this protein (Zulianello *et al*., 2000; Supattapone *et al*., 2001), does this imply that endocytosis is essential for the propagation of prion infection? Our results allow a more subtle mechanism; this motif may play an essential role in the assembly of an endocytic complex within non-raft membrane on the cell

surface. The involvement of the basic motif, and the N-terminal domain more generally, in the conversion of PrP^C could reside in its determination of the molecular environment of this protein on the cell surface rather than in directing endocytosis *per se*.

The diversity of membrane environment sampled by PrP^C may explain apparently contradictory results concerning the infection of PrP^C by exogenous PrP^{res}. Passage of prion infection between cells is optimally efficient if presented by direct cell contact between the infected cell and its target, i.e. by PrP^C and PrP^{res} being on opposed cell surfaces (Kanu *et al*., 2002). However, PrP^C within isolated lipid rafts is highly resistant to conversion to PrP^{res} in a non-cellular assay (Baron *et al*., 2002), and inhibition of sphingolipid synthesis in cells, depleting an essential raft component, increases the rate of conversion of PrP^C (Naslavsky *et al*., 1999). Both these findings suggest that the native conformation of PrP^C is protected within the raft environment. Perhaps it is PrP^C within the endocytic complex, and not that within rafts, that is susceptible to infection. Not only must the protein interactions of PrP^C be very different in these two environments, lipid interactions must also differ significantly (Morris *et al*., 2003). On neurons, raft sphingolipids are heavily glycosylated, forming a hydrophilic glycocalx above the membrane that would help stabilize the hydrophilic, α-helical form of PrP^C; the surface outside rafts is dominated by non-glycosylated phosphatidylcholine that presents a more hydrophobic face to membrane proteins, possibly favouring the hydrophobic PrP^{res} form.

Materials and methods

Labels, plasmids and biochemistry

PrP^C was detected with Fab preparations of monoclonal SAF34 (Demart *et al*., 1999) and sheep $MoP\alpha^1S$ (Ford *et al*., 2002a); both gave identical patterns of labelling, remained bound at pH as low as 4.0, and were used interchangeably. 3F4-tagged PrP was detected with monoclonal 3F4 (DAKO) (Kascsak *et al*., 1987), and Thy-1 with monoclonal Fabs as before (Tiveron *et al*., 1994). Biotinylated or Texas red-coupled Tf were from Molecular Probes, and LDL was from Sigma. Their production, coupling and the steps taken to avoid multivalent binding are described in the Supplementary data, along with the construction of plasmids expressing mutant forms of PrP. Labelling of AP2 (Oncogene Inc.) was detected with 10 nm anti-Ig-coated beads (British BioCell Ltd). Immunoprecipitation and raft isolation are described in the Supplementary data.

Cells and transfections

Mouse neuroblastoma N2a cells expressing endogenous mouse PrP^C were maintained in 20 mM HEPES/Dulbecco's modified Eagle's medium (DMEM) (Gibco-BRL) with 10% fetal calf serum. Cells were transfected with expression vectors using Lipofectamine, selected in 1 mg/ml G418 (both Gibco-BRL) and sorted on a Cytomation multilaser flow cytometer to obtain polyclonal populations of cells stably expressing defined levels of the transfected proteins. Adult mouse sensory neurons (Madore *et al*., 1999) were assayed after 2–3 days *in vitro.*

Endocytosis assays and fluorescent analysis

Endocytosis assays and fluorescent analysis are described in detail in the Supplementary data. Briefly, cells were serum starved for 2 h in HEPES/DMEM, pre-labelled at 10°C for 30 min with Fabs, with Tf or LDL added for the last 10 min; the coverslips were then placed in a 37°C incubator for the period indicated, fixed and processed for light or electron microscopy. Fluorescent images were collected with a Hamamatsu Orca ER camera on a Zeiss Axiovert 100 microscope using Improvision (Warwick, UK) OpenLab 2.0.5 software directing a piezo *z*-axis drive in 200 nm steps with filter wheel control of excitation and Pinkel filter set (Omega Optical) to handle emitted wavelengths. Images were volume deconvolved and passed to Volocity (Improvision) for three-dimensional analysis. For electron microscopy, grids were viewed in a Hitachi 7600 at 75 kV with images collected digitally. Significance of data was assessed by paired two-tailed *t*-tests or analysis of variance with Fisher's protected LSD as appropriate.

Supplementary data

Supplementary data are available at *The EMBO Journal* Online.

Acknowledgements

We thank Catriona Graham, Ken Brady, Susan Hall and TiJesunimi Abiola for their help at many stages of this work, Chris Birkett, Alan Bennett and Sylvain Lehmann for cells/constructs, Wayne Turnbull and the Department of Immunobiology for flow cytometry, Louise Armstrong (Improvision) for extensive assistance with image analysis, and the BBSRC (BS3081370), MRC (G839:53768) and EU (B104-CT98-6055) for funding.

References

Alonso,D.O.V., DeArmond,S.J., Cohen,F.E. and Daggett,V. (2001) Mapping the early steps in the pH-induced conformational conversion of the prion protein. *Proc. Natl Acad. Sci. USA*, **98**, 2985–2989.

Bamezai,A., Goldmacher,V.S. and Rock,K.L. (1992) Internalization of glycosyl-phosphatidylinositol (GPI)-anchored lymphocyte proteins. II. GPI-anchored and transmembrane molecules internalize through distinct pathways. *Eur. J. Immunol.*, **22**, 15–21.

Baron,G.S., Wehrly,K., Dorward,D.W., Chesebro,B. and Caughey,B. (2002) Conversion of raft associated prion protein to the protease-resistant state requires insertion of PrP-res (PrP(Sc)) into contiguous membranes. *EMBO J.*, **21**, 1031–1040.

Borchelt,D.R., Taraboulos,A. and Prusiner,S.B. (1992) Evidence for synthesis of scrapie prion proteins in the endocytic pathway. *J. Biol. Chem.*, **267**, 16188–16199.

Brown,D.A. and Rose,J.K. (1992) Sorting of GPI-anchored proteins to glycolipid-enriched membrane subdomains during transport to the apical cell surface. *Cell*, **68**, 533–544.

Brown,D.R. (2001) Prion and prejudice: normal protein and the synapse. *Trends Neurosci.*, **24**, 85–90.

Büeler,H., Aguzzi,A., Sailer,A., Greiner,R.-A., Autenried,P., Aguet,M. and Weissmann,C. (1993) Mice devoid of PrP are resistant to scrapie. *Cell*, **73**, 1339–1347.

Caughey,B. and Raymond,G.J. (1991) The scrapie-associated form of PrP is made from a cell surface precursor that is both protease- and phospholipase-sensitive. *J. Biol. Chem.*, **266**, 18217–18223.

Caughey,B., Raymond,G.J., Ernst,D. and Race,R.E. (1991) N-terminal truncation of the scrapie-associated form of PrP by lysosomal protease(s): implications regarding the site of conversion of PrP to the protease-resistant state. *J. Virol.*, **65**, 6597–6603.

Caughey,B., Raymond,G.J., Callahan,M.A., Wong,C., Baron,G.S. and Xiong,L.W. (2001) Interactions and conversions of prion protein isoforms. *Adv. Protein Chem.*, **57**, 139–169.

Chatterjee,S., Smith,E.R., Hanada,K., Stevens,V.L. and Mayor,S. (2001) GPI anchoring leads to sphingolipid-dependent retention of endocytosed proteins in the recycling endosomal compartment. *EMBO J.*, **20**, 1583–1592.

Chesebro,B. (1998) BSE and prions: uncertainties about the agent. *Science*, **279**, 42–43.

Czekay,R.P., Kuemmel,T.A., Orlando,R.A. and Farquhar,M.G. (2001) Direct binding of occupied urokinase receptor (uPAR) to LDL receptor-related protein is required for endocytosis of uPAR and regulation of cell surface urokinase activity. *Mol. Biol. Cell*, **12**, 1467–1479.

Damke,H., Baba,T., van der Bliek,A.M. and Schmid,S.L. (1995) Clathrin-independent pinocytosis is induced in cells overexpressing a temperature-sensitive mutant of dynamin. *J. Cell Biol.*, **131**, 69–80.

Demart,S. *et al*. (1999) New insight into abnormal prion protein using monoclonal antibodies. *Biochem. Biophys. Res. Commun.*, **265**, 652–657.

Fivaz,M., Vilbois,F., Thurnheer,S., Passquali,C., Abrami,L., Bickel,P.E., Parton,R.G. and van der Goot,F.G. (2002) Differential sorting and fate of endocytosed GPI-anchored proteins. *EMBO J.*, **21**, 3989–4000.

Ford,M.L., Burton,L.J., Li,H., Graham,C.H., Frobert,Y., Grassi,J.,

Hall,S.M. and Morris,R.J. (2002a) A marked disparity between the expression of prion protein and its message by neurons of the central nervous system. *Neuroscience*, **111**, 533–551.

Ford,M.L., Burton,L.J., Morris,R.J. and Hall,S.M. (2002b) Selective expression of prion protein in peripheral tissues of the adult mouse. *Neuroscience*, **113**, 177–192.

Gagescu,R., Demaurex,N., Parton,R.G., Hunziker,W., Huber,L.A. and Gruenberg,J. (2000) The recycling endosome of Madin–Darby canine kidney cells is a mildly acidic compartment rich in raft components. *Mol. Biol. Cell*, **11**, 2775–2791.

Gilbert,I. and Rudyk,H. (1999) Inhibitors of protease-resistant prion formation. *Intern. Antiviral News*, **7**, 78–82.

Harris,D.A. (1999) Cellular biology of prion diseases. *Clin. Microbiol. Rev.*, **12**, 429–444.

Hill,A.F., Antoniou,M. and Collinge,J. (1999) Protease-resistant prion protein produced *in vitro* lacks detectable infectivity. *J. Gen. Virol.*, **80**, 11–14.

Husemann,J., Loike,J.D., Anankov,R., Febbraio,M. and Silverstein,S.C. (2002) Scavenger receptors in neurobiology and neuropathology: their role on microglia and other cells of the nervous system. *Glia*, **40**, 195–205.

Kaneko,K., Vey,M., Scott,M., Pilkuhn,S., Cohen,F.E. and Prusiner,S.B. (1997) COOH-terminal sequence of the cellular prion protein directs subcellular trafficking and controls conversion into the scrapie isoform. *Proc. Natl Acad. Sci. USA*, **94**, 2333–2338.

Kanu,N., Imokawa,Y., Drechsel,D.N., Williamson,R.A., Birkett,C.R., Bostock,C.J. and Brockes,J.P. (2002) Transfer of scrapie prion infectivity by cell contact in culture. *Curr. Biol.*, **12**, 523–530.

Kascsak,R.J., Rubenstein,R., Merz,P.A., Tonna-DeMasi,M., Fersko,R., Carp,R.I., Wisniewski,H.M. and Diringer,H. (1987) Mouse polyclonal and monoclonal antibody to scrapie-associated fibril proteins. *J. Virol.*, **61**, 3688–3693.

Lamaze,C., Dujeancourt,A., Baba,T., Lo,C.G., Benmerah,A. and Dautry-Varsat,A. (2001) Interleukin 2 receptors and detergent-resistant membrane domains define a clathrin-independent endocytic pathway. *Mol. Cell*, **7**, 661–671.

Lemansky,P., Fatemi,S.H., Gorican,B., Meyale,S., Rossero,R. and Tartakoff,A.M. (1990) Dynamics and longevity of the glycolipid-anchored membrane protein, Thy-1. *J. Cell Biol.*, **110**, 1525–1531.

Madore,N., Smith,K.L., Graham,C.H., Jen,A., Brady,K., Hall,S. and Morris,R. (1999) Functionally different GPI proteins are organised in different domains on the neuronal surface. *EMBO J.*, **18**, 6917–6926.

Magalhaes,A.C., Silva,J.A., Lee,K.S., Martins,V.R., Prado,V.F., Ferguson,S.S.G., Gomez,M.V., Brentani,R.R. and Prado,M.A.M. (2002) Endocytic intermediates involved with the intracellular trafficking of a fluorescent cellular prion protein. *J. Biol. Chem.*, **277**, 33311–33318.

Marella,M., Lehmann,S., Grassi,J. and Chabry,J. (2002) Filipin prevents pathological prion protein accumulation by reducing endocytosis and inducing cellular PrP release. *J. Biol. Chem.*, **277**, 25457–25464.

Matter,K., Yamamoto,E.M. and Mellman,I. (1994) Structural requirements and sequence motifs for polarized sorting and endocytosis of LDL and Fc receptors in MDCK cells. *J. Cell Biol.*, **126**, 991–1004.

Mayor,S., Sabharanjak,S. and Maxfield,F.R. (1998) Cholesterol-dependent retention of GPI-anchored proteins in endosomes. *EMBO J.*, **17**, 4626–4638.

McBride,P.A., Wilson,M.I., Eikelenboom,P., Tunstall,A. and Bruce,M.E. (1998) Heparan sulfate proteoglycan is associated with amyloid plaques and neuroanatomically targeted PrP pathology throughout the incubation period of scrapie-infected mice. *Exp. Neurol.*, **149**, 447–454.

Morillas,M., Swiezicki,W., Gambetti,P. and Surewicz,W.K. (1999) Membrane environment alters the conformational structure of the recombinant human prion protein. *J. Biol. Chem.*, **274**, 36859–36865.

Morris,R. (1992) Thy-1, the enigmatic extrovert on the neuronal surface. *BioEssays*, **14**, 715–722.

Morris,R.J., Cox,H.M., Mombelli,E. and Quinn,P.J. (2003) Rafts, little caves and large potholes: how lipid structure interacts with membrane proteins to create functionally diverse membrane environments. In Quinn,P.J. (ed.), *Membrane Dynamics and Domains*. Kluwer Academic/Plenum Publishers, London, UK, in press.

Naslavsky,N., Shmeeda,H., Friedlander,G., Yanai,A., Futerman,A.H., Barenholz,Y. and Taraboulos,A. (1999) Sphingolipid depletion increases formation of the scrapie prion protein in neuroblastoma cells infected with prions. *J. Biol. Chem.*, **274**, 20763–20771.

Nunziante,M., Gilch,S. and Schatzl,H.M. (2003) Essential role of the prion protein N terminus in subcellular trafficking and half-life of cellular prion protein. *J. Biol. Chem.*, **278**, 3726–3734.

Pan,T., Wong,B.S., Liu,T., Li,R., Petersen,R.B. and Sy,M.S. (2002) Cell-surface prion protein interacts with glycosaminoglycans. *Biochem. J.*, **368**, 81–90.

Pauly,P.C. and Harris,D.A. (1998) Copper stimulates endocytosis of the prion protein. *J. Biol. Chem.*, **273**, 33107–33110.

Perera,W.S. and Hooper,N.M. (2001) Ablation of the metal ion-induced endocytosis of the prion protein by disease-associated mutation of the octarepeat region. *Curr. Biol.*, **11**, 519–523.

Prusiner,S.B. (1998) Prions. *Proc. Natl Acad. Sci. USA*, **95**, 13363–13383.

Puri,V., Watanabe,R., Singh,R.D., Dominguez,M., Brown,J.C., Wheatley,C.L., Marks,D.L. and Pagano,R.E. (2001) Clathrin-dependent and -independent internalization of plasma membrane sphingolipids initiates two Golgi targeting pathways. *J. Cell Biol.*, **154**, 535–547.

Rijnboutt,S., Jansen,G., Posthuma,G., Hynes,J.B., Schornagel,J.H. and Strous,G.J. (1996) Endocytosis of GPI-linked membrane folate receptor-α. *J. Cell Biol.*, **132**, 35–47.

Rivera-Milla,E., Stuermer,C.A. and Malaga-Trillo,E. (2003) An evolutionary basis for scrapie disease: identification of a fish prion mRNA. *Trends Genet.*, **19**, 72–75.

Sabharanjak,S., Sharma,P., Parton,R.G. and Mayor,S. (2002) GPI-anchored proteins are delivered to recycling endosomes via a distinct cdc42-regulated, clathrin-independent pinocytic pathway. *Dev. Cell*, **2**, 411–423.

Sanan,D.A. and Anderson,R.G. (1991) Simultaneous visualization of LDL receptor distribution and clathrin lattices on membranes torn from the upper surface of cultured cells. *J. Histochem. Cytochem.*, **39**, 1017–1024.

Sanghera,N. and Pinherio,T.J.T. (2002) Binding of prion protein to lipid membranes and implications for prion conversion. *J. Mol. Biol.*, **315**, 1241–1256.

Shogomori,H. and Futerman,A.H. (2001) Cholera toxin is found in detergent-insoluble rafts/domains at the cell surface of hippocampal neurons but is internalized via a raft-independent mechanism. *J. Biol. Chem.*, **276**, 9182–9188.

Shyng,S.-L., Huber,M.T. and Harris,D.A. (1993) A prion protein cycles between the cell surface and an endocytic compartment in cultured neuroblastoma cells. *J. Biol. Chem.*, **268**, 15922–15928.

Shyng,S.-L., Heuser,J.E. and Harris,D.A. (1994) A glycolipid-anchored prion protein is endocytosed via clathrin-coated pits. *J. Cell Biol.*, **125**, 1239–1250.

Shyng,S.-L., Moulder,K.L., Lesko,A. and Harris,D.A. (1995a) The N-terminal domain of a glycolipid-anchored prion protein is essential for its endocytosis via clathrin-coated pits. *J. Biol. Chem.*, **270**, 14793–14800.

Shyng,S.L., Lehmann,S., Moulder,K.L. and Harris,D.A. (1995b) Sulfated glycans stimulate endocytosis of the cellular isoform of the prion protein, PrPC, in cultured cells. *J. Biol. Chem.*, **270**, 30221–30229.

Sieczkarski,S.B. and Whittaker,G.R. (2002) Influenza virus can enter and infect cells in the absence of clathrin-mediated endocytosis. *J. Virol.*, **76**, 10455–10464.

Simonic,T., Duga,S., Strumbo,B., Asselta,R., Ceciliani,F. and Ronchi,S. (2000) cDNA cloning of turtle prion protein. *FEBS Lett.*, **469**, 33–38.

Simons,K. and Ikonen,E. (1997) Functional rafts in cell membranes. *Nature*, **387**, 569–572.

Stahl,N., Borchelt,D.R., Hsiao,K. and Prusiner,S.B. (1987) Scrapie prion protein contains a phosphatidylinositol glycoplipid. *Cell*, **51**, 229–240.

Strumbo,B., Ronchi,S., Bolis,L.C. and Simonic,T. (2001) Molecular cloning of the cDNA coding for *Xenopus laevis* prion protein. *FEBS Lett.*, **508**, 170–174.

Supattapone,S., Muramoto,T., Legname,G., Mehlhorn,I., Cohen,F.E., DeArmond,S.J., Prusiner,S.B. and Scott,M.R. (2001) Identification of two prion protein regions that modify scrapie incubation time. *J. Virol.*, **75**, 1408–1413.

Taraboulos,A., Scott,M., Semenov,A., Avrahami,D., Laszlo,L., Prusiner,S.B. and Avraham,D. (1995) Cholesterol depletion and modification of COOH-terminal targeting sequence of the prion protein inhibit formation of the scrapie isoform. *J. Cell Biol.*, **129**, 121–132.

Tiveron,M.C., Nosten-Bertrand,M., Jani,H., Garnett,D., Hirst,E.M.A., Grosveld,F. and Morris,R.J. (1994) The mode of anchorage to the cell surface determines both the function and membrane location of Thy-1 glycoprotein. *J. Cell Sci.*, **107**, 1783–1796.

Triantafilou,M. and Triantafilou,K. (2002) Lipopolysaccharide recognition: CD14, TLRs and the LPS-activation cluster. *Trends Immunol.*, **23**, 301–304.

Vilhardt,F., Nielsen,M., Sandvig,K. and van Deurs,B. (1999) Urokinase-type plasminogen activator receptor is internalized by different mechanisms in polarized and nonpolarized Madin–Darby canine kidney epithelial cells. *Mol. Biol. Cell*, **10**, 179–195.

Warner,R.G., Hundt,C., Weiss,S. and Turnbull,J.E. (2002) Identification of the heparan sulphate binding sites in the cellular prion protein. *J. Biol. Chem.*, **277**, 18421–18430.

Weissmann,C., Raeber,A.J., Montrasio,F., Hegyi,I., Frigg,R., Klein,M.A. and Aguzzi,A. (2001) Prions and the lymphoreticular system. *Philos. Trans. R. Soc. Lond. B Biol. Sci.*, **356**, 177–184.

Wettey,F.R., Hawkins,S.F., Stewart,A., Luzio,J.P., Howard,J.C. and Jackson,A.P. (2002) Controlled elimination of clathrin heavy-chain expression in DT40 lymphocytes. *Science*, **297**, 1521–1525.

Zulianello,L., Kaneko,K., Scott,M., Erpel,S., Han,D., Cohen,F.E. and Prusiner,S.B. (2000) Dominant-negative inhibition of prion formation diminished by deletion mutagenesis of the prion protein. *J. Virol.*, **74**, 4351–4360.

Received May 27, 2002; revised May 6, 2003;
accepted May 20, 2003